A simulation-based assessment of the relation between Stone Age sites and relative sea-level change along the Norwegian Skagerrak coast

Isak Roalkvam[1,*]

07 December, 2021

[1] University of Oslo

[*] Correspondence: Isak Roalkvam <isak.roalkvam@iakh.uio.no>

1 Introduction

The post-glacial relative sea-level fall that characterises large areas of Fennoscandia is fundamental to its archaeology. This follows not only from the dramatic changes to the landscape that this process has represented throughout prehistory, but also from the fact that if archaeological phenomena were situated close to the contemporary shoreline when they were in use, a reconstruction of the trajectory of shoreline displacement can be used to date these phenomena based on their altitude relative to the present day sea-level. This method, also called shoreline dating, has long history of use in the region and is frequently applied to assign an approximate date to diverse archaeological phenomena such as rock art, grave cairns, various harbour and sea-side constructions and, as is the focus of this study, Stone Age sites (e.g. Berg-Hansen, 2009; Bjerck, 2005; Sognnes, 2003; Tallavaara and Pesonen, 2020).

The close association between Norwegian Stone Age sites located in coastal regions and prehistoric shorelines was firmly established by the geologist W.C. Brøgger in 1905 (see the review by MacCurdy (1906) for an early mention in English). Shoreline dating has been fundamental to Stone Age research in Norway ever since (e.g. Berg-Hansen, 2009; Bjerck, 1990; Mjærum, 2018). The method is used both independently and to compliment the dating of sites where other sources of temporal data such as typological indicators or radiometric dates are either limited or not available. Given the coarse and fuzzy resolution of established typological frameworks, the vast amount of surveyed sites that only contain generic lithic debitage that could hail from any part of the period, and as the conditions for the preservation of organic material is typically poor in Norway, dating with reference to shoreline displacement is often the only and most accurate method by which one can hope to date the sites. Shoreline dating is consequently fundamental to our understanding of the Norwegian Stone Age. This is both because it is fundamental to the temporal framework on which our understanding of the period is based, but also because the method is only applicable so long as the societies in question have continuously settled on or close to the contemporary shoreline. Consequently, adherence or deviation from this pattern also has major implications for the socio-economic foundations of the societies in question.

Despite its fundamental role for Norwegian Stone Age archaeology, the applicability of dating by reference to shoreline displacement has only been evaluated using relatively coarse methods. The aim of this paper is to provide a systematic and comprehensive review of the degree to which radiocarbon dates correspond with the dates informed by our current knowledge of shoreline displacement in a larger area of south-eastern Norway, using a more refined methodological approach. The goal is to quantify the degree to which the assumption of shore-bound settlement holds through the Stone Age. As presented in more detail below, this problem involves the combined evaluation of three major analytical dimensions. One is the questions of when the sites

were in use, the second pertains to the reconstruction of the contemporaneous sea-level, and the third follows from the fact that the relation between site and shoreline is inherently spatial. Taking inspiration from recent studies that have integrated various sources of spatio-temporal uncertainty through Monte Carlo simulation (e.g. Crema, 2012; Crema et al., 2010; Lewis, 2021), a similar approach is adopted here.

2 Background

Relative sea-level (RSL) can be defined as the mean elevation of the surface of the sea relative to land, or, more formally, the difference in elevation between the geoid and the surface of the Earth as measured from the Earth's centre (Shennan, 2015). Variation in this relative distance follow from a range of effects (e.g. Milne et al., 2009; Mörner, 1976). Of central importance here is eustasy and glacial istostasy. The eustatic sea-level is understood as the sea-level if the water has been evenly distributed across the Earth's surface without adjusting for variation in the rigidity of the Earth, its rotation, or the self-gravitation inherent to the water body itself (Shennan, 2015). The eustatic sea-level is mainly impacted by glaciation and de-glaciation, which can bind or release large amounts of water into the oceans, as well as by changes in the Earth's crust that impact the volume of ocean basins. Istostasy, on the other hand, pertains to adjustments in the crust to regain gravitational equilibrium relative to the underlying viscous mantle. This is often the result of glacial istostasy, which follows from glaciation and de-glaciation and corresponding loading and unloading of weight, as well as from erosion of the crust, which causes its weight to be redistributed. These effects thus causes the lithosphere to either subside due to increased weight, or to rebound and lift upwards due to lower weight (Milne, 2015).

Following the end of the Weichselian and the final retreat of the Fennoscandian Ice Sheet (e.g. Hughes et al., 2016; Stroeven et al., 2016), the isostatic rebound has been so severe that most areas of Norway have been subject to a continuous relative sea-level regression, despite corresponding eustatic sea-level rise (e.g. Lambeck et al., 1998; Svendsen and Mangerud, 1987). In other words, the RSL has been dropping throughout prehistory. As this process is the result of glacial loading, the rate of uplift is more severe towards the centre of the ice sheet. Thus, some areas on the outer coast have had a more stable RSL or been subject to marine transgression (e.g. Romundset et al., 2015; Svendsen and Mangerud, 1987). These conditions are directly reflected in the archaeological record. In areas where the sea-level has been stable over longer periods of time, people have often reused the coastal site locations multiple times and over long time-spans, creating a mix of settlement events that are difficult to disentangle (Reitan and Berg-Hansen, 2009). Transgression phases, on the other hand, can lead to complete destruction of the sites, or bury them in marine sediments, leading to a hiatus in the archaeological record for certain sub-phases in the impacted areas (Bjerck, 2008). Comparatively, given a continuous and still ongoing shoreline regression from as high as c. 220 m above present sea-level in the inner Oslo fjord, any one location in south-eastern Norway has only been shore-bound within a relatively limited time-span, and the sites have not been impacted by any transgressions (Hafsten, 1983, 1957; Sørensen, 1979). This makes the region especially useful for evaluating the assumption of a shore-bound settlement over a long and continuous time-span.

Based on the generally accepted premise that most Stone Age sites in south-eastern Norway located lower than the marine limit were situated on or close to the contemporaneous shoreline, it is common to err on the side of a shore-bound site location unless there is strong evidence to suggest otherwise. This is for example common in survey projects, which are often guided by a both a digital and mental reconstruction of past sea-levels. Similarly, following an excavation, if typological indicators in the assemblages correspond with available shoreline displacement curves it is common to assume a shore-bound site location, even if the possible time-span provided by the typological indicators are too wide to decisively verify this. It is also common to combine this with a qualitative consideration of the landscape surrounding the sites, and an evaluation of the degree to which the site location would have been sensible if the site was not shore bound (e.g. Jaksland, 2014; Nummedal, 1923). This can for example pertain to accessibility. If the site is situated on a ledge in a steep and jagged area of the present day landscape, or if it would have been located on an island when the sea-level was higher, it would make intuitive sense that the site was in use when the ocean reached closer to its elevation, as the site would have been accessible by means of watercraft.

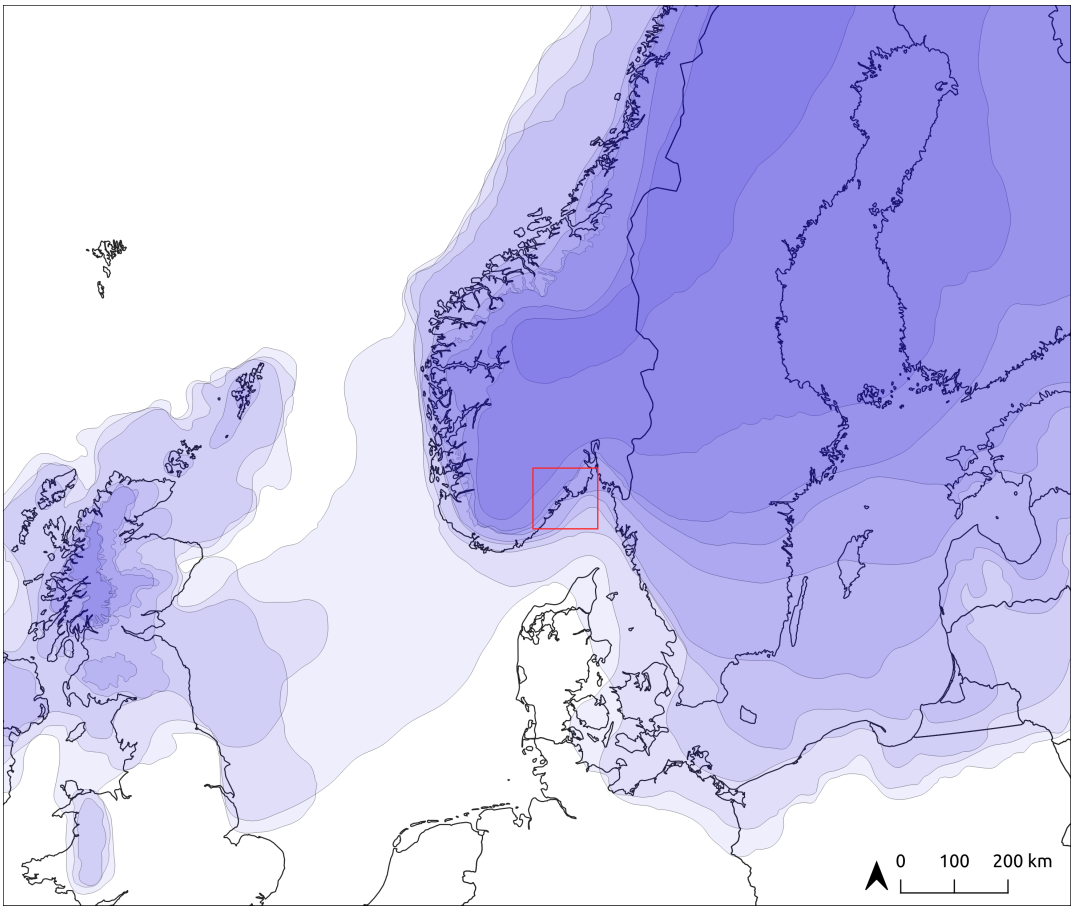

Figure 1: Deglaciation at 1000 year intervals from 19–10 ka (data from Hughes et al. 2016). The studyarea defined later in the text is given a red outline.

Although it appears that the arguments for such site locations are sensible and can for the most part be assumed to hold, comprehensive evaluations and attempts at quantification of this tendency are fewer, and are typically conducted on a site-by-site or project-by-project basis, meaning the fundamental basis for assuming shore-bound site location is largely based on a mosaic of smaller scale investigations.

One of the more comprehensive evaluations of this relationship was done by Solheim and colleagues (Breivik et al. (2018); Solheim (2020)), who compared 102 ^{14}C-dates from 29 Mesolithic sites on the western side of the Oslo fjord to the displacement curve for the Larvik area. They found a overlap between the probability distribution of the radiocarbon dates with the shoreline displacement curve for 86.5% of the sites. However, where there was a discrepancy, the main occupation of the sites are still believed to have been shore-bound rather than associated with the deviating ^{14}C-dates. This is based on typological and technological characteristics of the assemblages. Whether these mismatches represent later shorter visits that are responsible for the younger radiocarbon dates, or whether they are entirely erroneous results of contamination can be difficult to evaluate. Here this will be entirely dependent on, and follow the discretion of the original excavation reports.

Other previous evaluations of the correspondence between dates informed by radiocarbon dates and shoreline dating have typically followed the same structure as that of Breivik et al. (2018), involving a visual inspection of radiocarbon probability distributions plotted against local shoreline displacement curves based on the elevation of the site (Åstveit, 2018; e.g. Solheim, 2020). This approach has a couple of limitations. First of all, the displacement curves are commonly applied directly to larger study areas, with only a couple of studies having taken the variable uplift-rates into account when performing this comparison (e.g. Fossum, 2020; Møller, 1987; **persson2008?**). Secondly, with this method, the wider the uncertainty range associated with either radiocarbon date or displacement curve, the higher the probability that the confidence intervals overlap, and the higher the probability that we conclude in favour of our hypothesis. This thus leads to an inferential framework that favours uncertainty, which is hardly desirable. In statistical terms this follows from the fact that while one cannot conclude that two dates are different if their confidence intervals overlap, this does not necessarily mean that they are the same. The question thus necessitates a flip from a null-hypothesis of no significant difference, to one of equivalence (e.g. Lakens et al., 2018), as the question of interest is effectively one of synchroneity between events (cf. Parnell et al., 2008). Another limitation of this often employed method is that it only takes into account the vertical distance between the sites and the sea-level. While this is the main parameter of interest for shoreline dating, the practical implications of a vertical difference in RSL will be highly dependent on local topography and bathymetry. RSL-change can have more dramatic consequences in a landscape characterised by a low relief, as the horisontal displacement of the shoreline will be greater. Taking the spatial nature of the relationship between site and shoreline into account will consequently help get more directly at the behavioural dimension of the relation between site and shore line, and move the analysis beyond a purely instrumental consideration of the applicability of shoreline dating. Suggested ways to help mitigate and integrate the issues presented above into to the analysis are presented in the methods section.

3 Data

All data and R programming code (R Core Team, 2021) required to run the analyses, as well as the derived data are freely available in an online repository at https://osf.io/7f9su/, organised as a digital research compendium following Marwick et al. (2018). The dataset is slightly more extensive than what is directly utilised in the study, and includes excavated sites without ^{14}C-dates, as well as ^{14}C-dates to periods other than the Stone Age.

To get at the relationship between sites and contemporaneous shoreline, the analysis is dependent on a study area with good control of the trajectory of prehistoric shoreline displacement. While there is displacement data available for other areas of south-eastern Norway (e.g. Hafsten, 1957; Sørensen, 1999, 1979), considerable methodological developments in recent years means that the most well-established displacement curves are from the region stretching from Horten county in the north-east, to Arendal in the south-west. This area has

newly compiled displacement curves for Horten (**romundset2021?**), Larvik (Sørensen et al., 2014a, 2014b), Tvedestrand (Romundset et al., 2018; Romundset, 2018), and Arendal (Romundset, 2018).

The employed shoreline displacement curves are all based on the so-called isolation basin method (Romundset et al., 2011). This involves extracting cores from a series of basins located beneath the marine limit situated on bedrock in a constrained area of the landscape, and dating the transition from marine to lacustrine sediments in the cores. Each curve is thus construed from a series of cored basins located at different elevations, each representing a high precision sea-level index point. The confidence bands of the displacement curves and their trajectory are quite complex constructs, and are the integrated result of both expert knowledge and more objectively quantifiable parameters. The reason for this is in part that the curves do not only contain uncertainty as related to radiometric dates, which are well defined, but also hold potential error as related to the interpretation and analysis of sediment cores, the nature and condition of the basin outlets, the adjustment to a common isobase based on the direction and gradient in rebound intensity, to name but a few (Romundset et al., 2019, e.g. 2011). For more details and evaluations done for the compilation of each curve, the reader is therefore referred to the individual publications (see above).

The archaeological data compiled for the analysis consists of all excavated Stone Age sites with available spatial data from the coastal region between Horten county in the north-east, to Arendal in the south-west (Figure 2). These number a total 154 sites. Of these 90 sites are associated with the total of 530 radiocarbon dates. In turn, 68 sites are related to the 247 radiocarbon dates that fall within the Stone Age (9500–1700 BCE) with 95 % probability. These sites form the basis for the analysis. Spatial data in the form of site limits and features, as defined by the excavating archaeologists, were retrieved from local databases at the Museum of Cultural History—the institution responsible for archaeological excavations in the region. In the compiled dataset, each radiocarbon date has been associated with the site features or excavation unit from where they originate, or, where these weren't available, the spatial limit of the entire site. Due to somewhat variable practices between excavations, what available spatial geometry best represents the site limit was decided based on an evaluation of the excavation reports. This means that the limits are variably given as area de-turfed before excavation, area stripped with excavator following the excavation, manually excavated area, or convex hull polygons generated around the site features.

[Table with sites]

The elevation data used for the analysis is a digital terrain model (DTM) freely available from the Norwegian Mapping Authority (**mapping2019?**). After evaluating the options I decided to use 10m resolution DTM rather than the higher-resolution 1m version. In addition to resulting is less processing time, the higher resolution elevation model is more vulnerable to smaller-scale modern disturbances that the 10m version is not impacted by. The 10m DTM is a down-sampled version of the 1m resolution DTM, which is based on aerial laser scanning using a minimum of two and up to five points per m^2 (**mapping2019?**).

4 Methods

The goal of this study is effectively to evaluate the spatial relationship between two phenomena, sites and shorelines, each associated with their own range of temporal uncertainty. The first task was therefore to ascribe likely date ranges and associated uncertainty to the two phenomena.

To take account of the gradient in the isostatic rebound, the shoreline displacement curves were adjusted to each site location by taking into account the distance to the closest isobase. This was done by for each site first finding the difference between the elevation values of the two closest displacement curves for each year along the entirety of the curves. Each value was then divided by the distance between the isobases. To find the adjusted displacement curve for a given site location, the distance between the site polygon and closest isobase was multiplied with the values for difference per meter. These values were then subtracted from the dsiplacement curve located to the south-west of the site. The result of this process is shown for an example site in Figure 3.

For the date ranges associated with the sites, all radiocarbon dates were first individually calibrated using

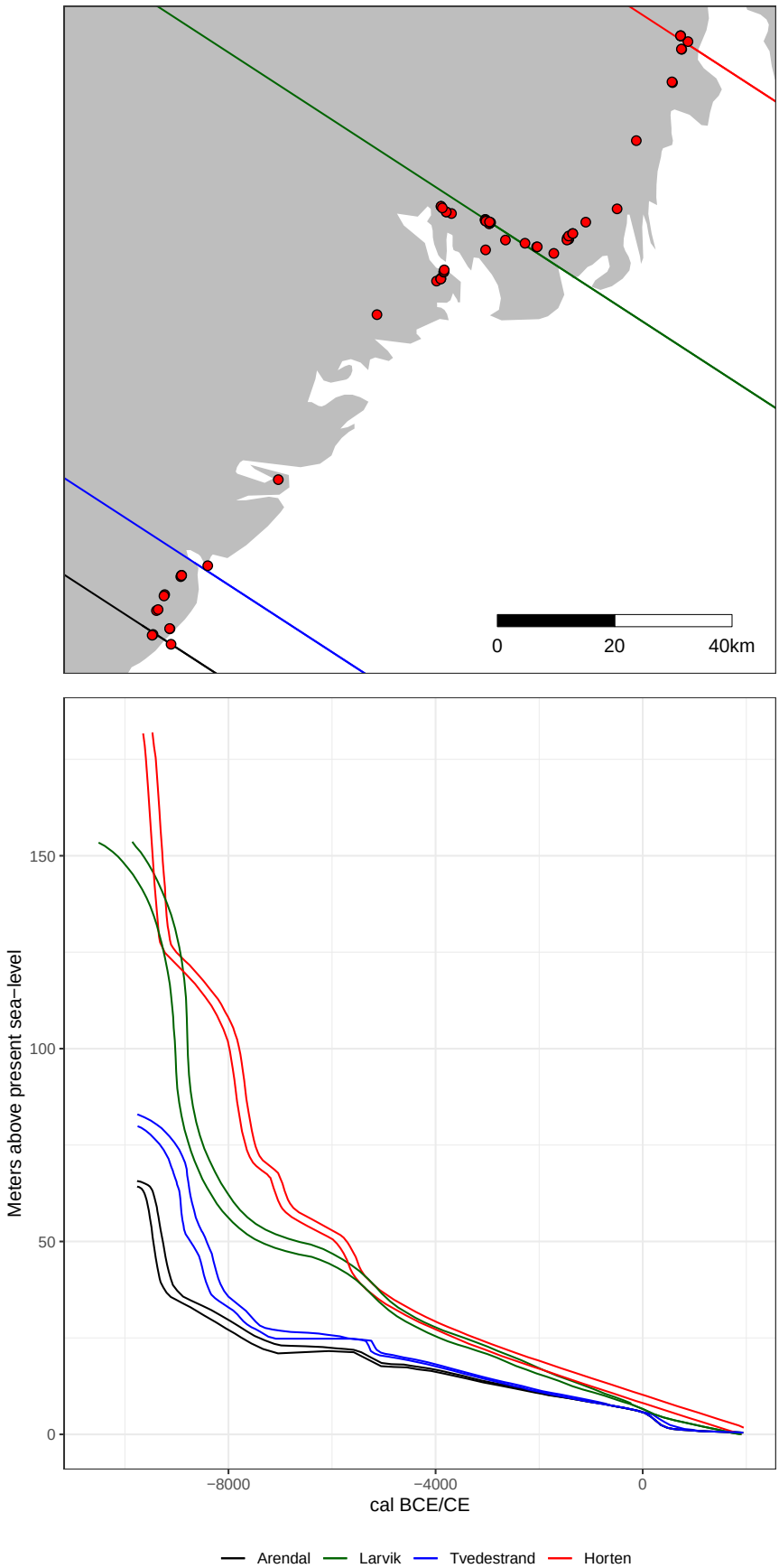

Figure 2: A) Distribution of the 68 analysed sites relative to the isobases of the displacement curves. The isobases have a direction of 327 ° (Romundset el al.2018), B) Displacement curves. Note the increasing steepness of the curves towards the north-east.

the IntCal20 calibration curve (Reimer et al., 2020) using OxCal v4.4.4 (Bronk Ramsey, 2009) through the oxcAAR package for R (Hinz et al., 2021). Radiocarbon dates associated with each site were then grouped if they overlapped with 99.7 % probability, meaning these were effectively taken to represent the same settlement phase. In the case were there are multiple dates believed to belong to a single phase, these were subjected to Bayesian modelling using the Boundary function in OxCal. Multiple phases at a single site were treated as independent of each other.

As the excavation of archaeological sites typically follow from residential and commercial development, as well as the expansion of infrastructure, the area immediately surrounding the sites have sometimes been severely impacted by modern disturbances. In addition to employing 10m resolution DTM to alleviate some of these issues, this also necessitated some additional editing of the elevation raster. This involved manually defining the extent of problem areas such as railways, highways, quarries and the like. The DTM values on these were then set to missing, and new elevation values were interpolated from the surrounding terrain. This was done using regularised spline interpolation with tension (e.g. Conolly, 2020), using the default settings of r.fillnulls from GRASS GIS in R through the package rgrass7 (Bivand, 2021). In addition to code and original spatial data being available in the research compendium for this paper, it has also been noted in the supplementary material when the area surrounding a site has been edited in this manner.

Armed with a likely date range for the occupation(s) of each site, an estimated trajectory of relative sea-level change at that location, and an DTM edited to remove substantial modern disturbances, the simulations were performed. A single simulation run involved first drawing a single year from the posterior density estimate of a given occupation phase of a site (Figure 4). This year then has a corresponding likely elevation range for the contemporaneous shoreline from which an elevation value was drawn uniformly, using intervals of 5cm. The sea-level was then raised to this elevation on the DTM by defining all elevation values at or below this altitude as missing. Polygons were then created from the resulting areas with missing values. The horisontal distance was then found by measuring the shortest distance between site and sea polygons, and the vertical distance by subtracting the elevation of the sea-level from the lowest elevation of the site polygon. The topographic distance between site and sea was also found by measuring the shortest distance while taking into account the slope of the terrain on the DTM. This was done using the topoDistance package for R (Wang, 2019). The topographic distance was measured between site polygon and the horisontally closest point on the shoreline. The shortest topographic path was found using the Queen's case neighbourhood of eight cells (Conolly and Lake, 2006). In the case where the sea-polygons intersects the site polygon, all distance measures were set to zero. In the case that the sea-polygon completely contain the site, the horisontal and topographic distance measures were made negative, and the vertical distance was instead measured to the highest point on the site polygon. While it is safe to assume that an archaeological site was not occupied when it was located beneath sea-level, a negative result can reflect the inherent uncertainty in this procedure, and might also help identify discrepancies in displacement data or radiocarbon dates. Negative values where therefore retained.

This process was repeated 1000 times for each phase for each site. The choice of 1000 simulation runs follows from an evaluation of when the mean distances between site and shoreline converged when running 5000 iterations of the simulation on the site Hovland 5. Hovland 5 was chosen for this evuluation as it has a fairly uncertain date range, and is located in area of quite complex topography. At 1000 simulation runs the analysis of each site ranged from hours to a couple of days, depending on the distance to the simulated shorelines and the necessary size of the window of analysis.

5 Results

The result of running the simulations across all sites are given in Figure 6. Overall, as is indicated by the measures for central tendency and the almost solid line along the 0 mark on the y-axes, most of the sites have been situated close to the shoreline when they were in use. When including all dates, also those that were believed to be erroneous in the original reports, some of the sites are situated considerable distances from the shoreline, as could be expected. To what degree these do in fact represent contamination is discussed further below. However, if one accepts the interpretation in the reports that these dates do not date the main occupation of the sites, the second row of Figure 6 gives considerable support to the notion that the

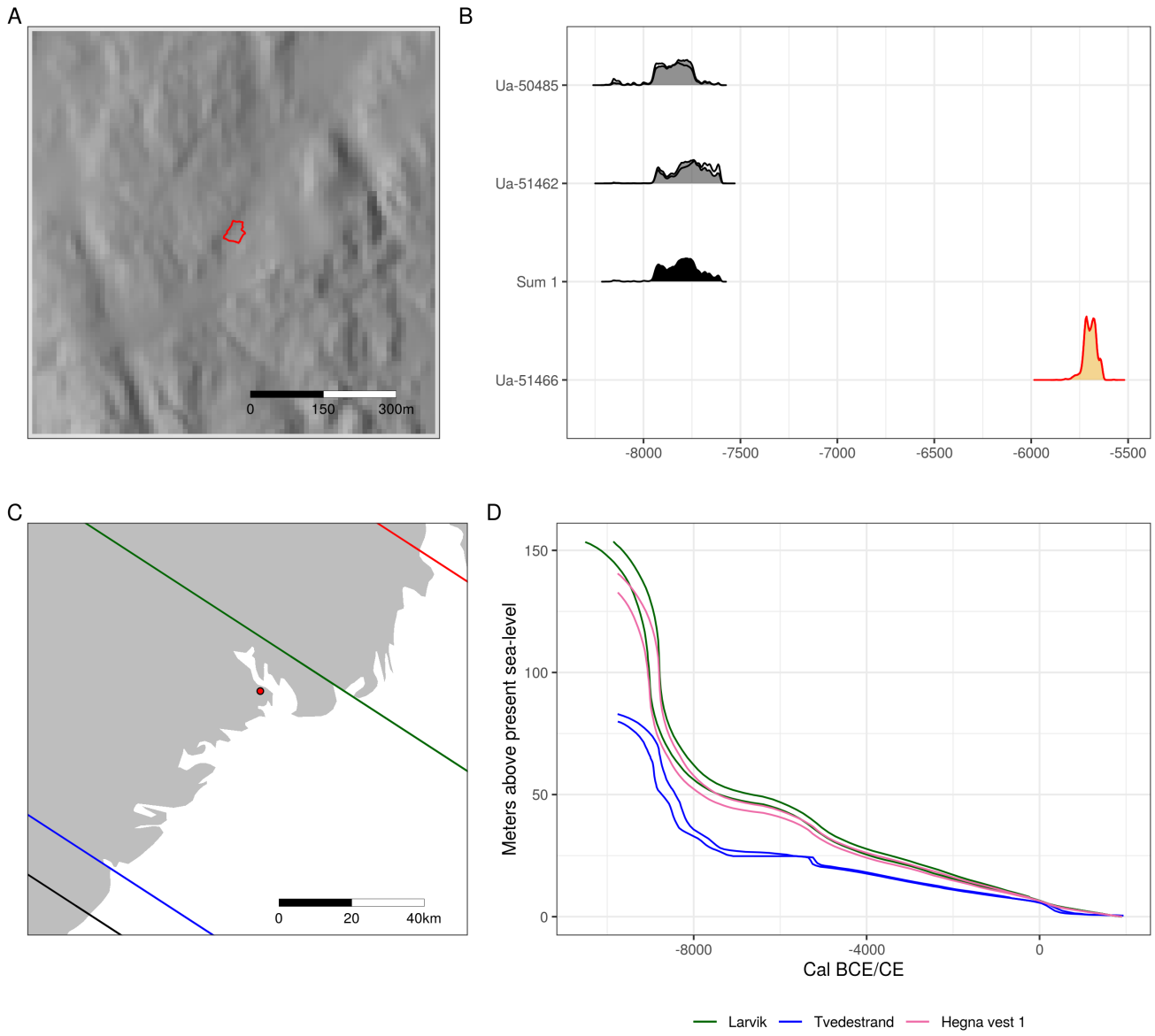

Figure 3: Example site Hegna vest 1 (Fossum 2017). A) Location of the site in the present day landscape. The red outline is the site limit. B) Radiocarbon dates associated with the site. Fill colour indicates what dates are assumed to belong to the same settlement phase. Multiple dates are modelled using the Boundary function in OxCal and then summed. The red outline indicates that the date does not match the typological indicators in the artefact assemblage of the site. C) The location of the site within the study area relative to isobases of the employed displacement curves. D) Displacement curve interpolated to the site location based on the distance between the site and the isobases of the two closest displacement curves.

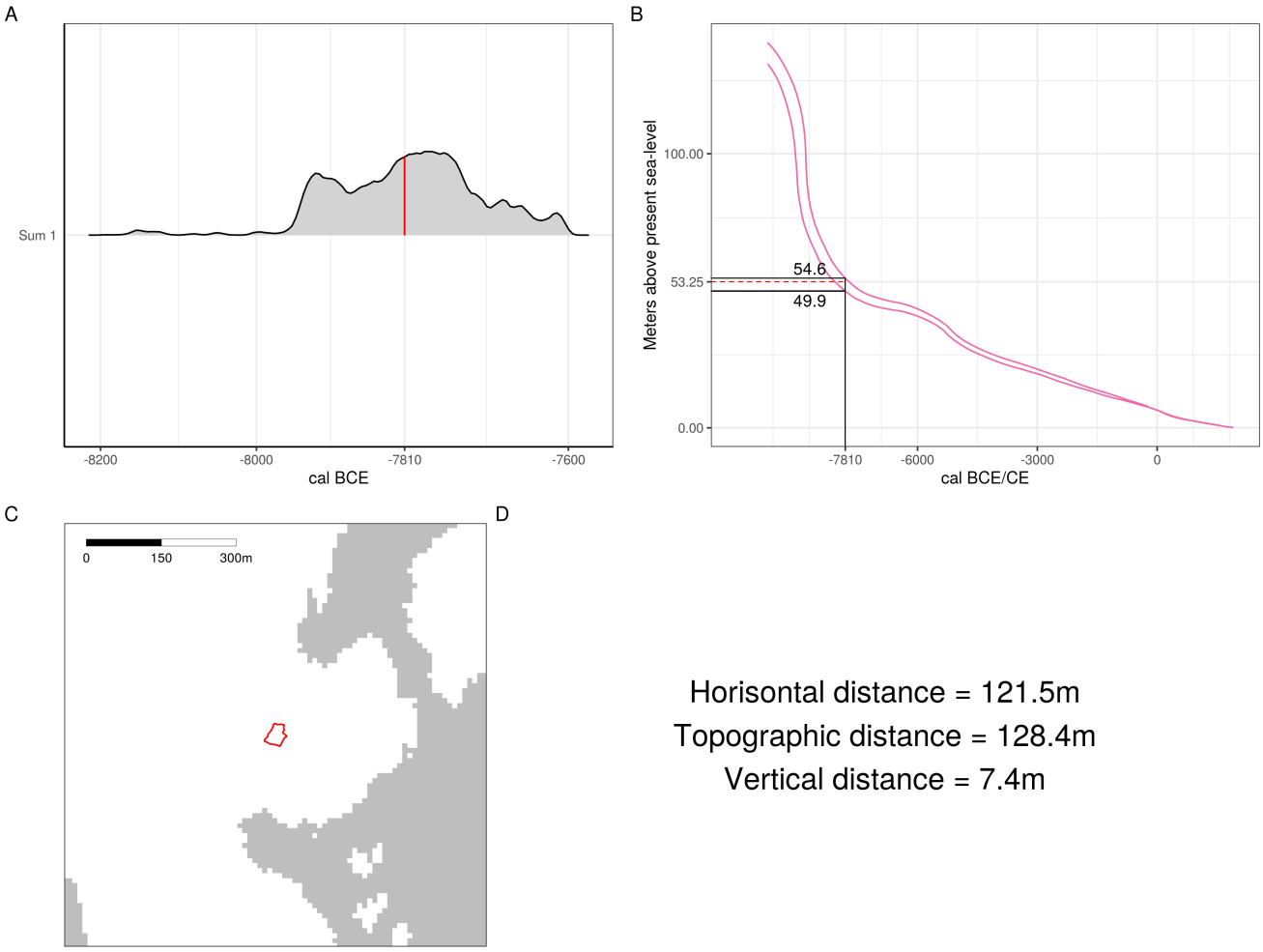

Figure 4: Example of a single simulation run on the site Hegna vest 1. A) The simulation starts by drawing a single year from the posterior density esimate. B) This then corresponds to an elevation range on the interpolated displacement curve. A single elevation is drawn uniformly from this range using 5cm intervals. C) The sea-level is then adjusted on the DTM to this elevation and the various distance mesaures are found. D) The numerical result of the simulation run.

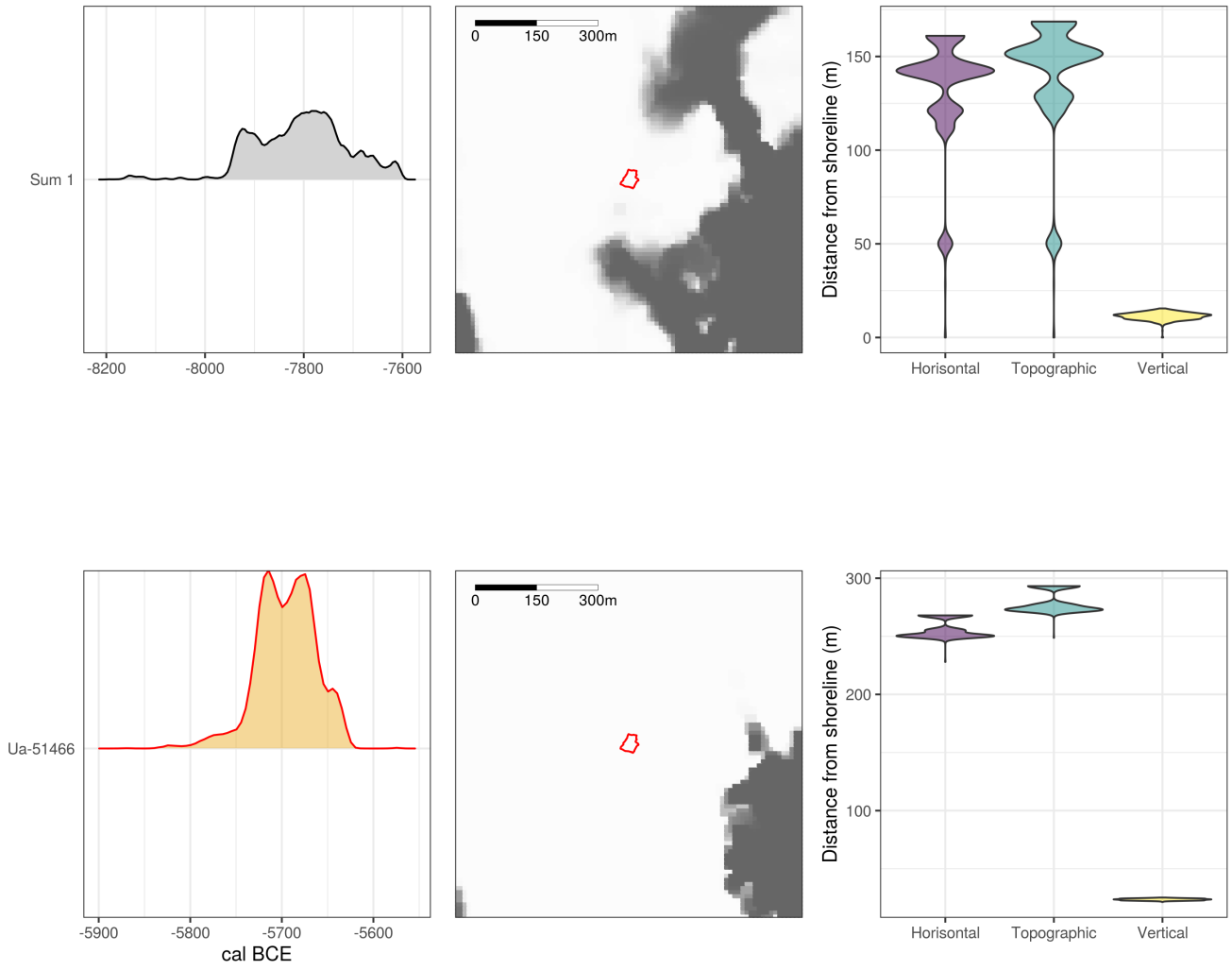

Figure 5: The result of 1000 simulation runs for each of the two grops of dates on the site Hegna vest 1. The first column of plots shows the radiocarbon probability density estimate from where dates were drawn during simulation. The second column displays the result of simulating the raised sea-level 1000 times. The darker the colour, the more times the sea-level was simulated to that location. The third column shows violin plots of the different distance measures across all simulations.

sites were in use when they were situated on or close to the contemporaneous shoreline. It is interesting to note the distance for some of the earliest sites, which appears somewhat high. This, however, can likely be explained as the result of the steepness of the displacement curves for the earliest part of the Holocene (Figure 2B), which leads the uncertainty in the ^{14}C-dates to give a wider possible elevation range for the sea-level. Another immediately striking result is the apparent deviation from the shoreline towards the end of the Stone Age. From around 2500 BCE several sites are situated a considerable distance from the shoreline, and while a couple remain horisontally and topograpchically close, they appear to be elevated a considerable distance from the sea-level, as indicated on the plot for vertical distance. This corresponds well with the literature, where the introduction of the Neolithic proper is seen as occurring around this time (Prescott, 2020; Solheim, 2021). With the transition from a predominantly hunter-gatherer lifeway to early agro-pastrolism, settlements in coastal areas are to be increasingly withdrawn from the shoreline. Given this, the results for the second row of Figure 6 is given again in Figure 7, excluding all simulation results younger than 2500 BCE.

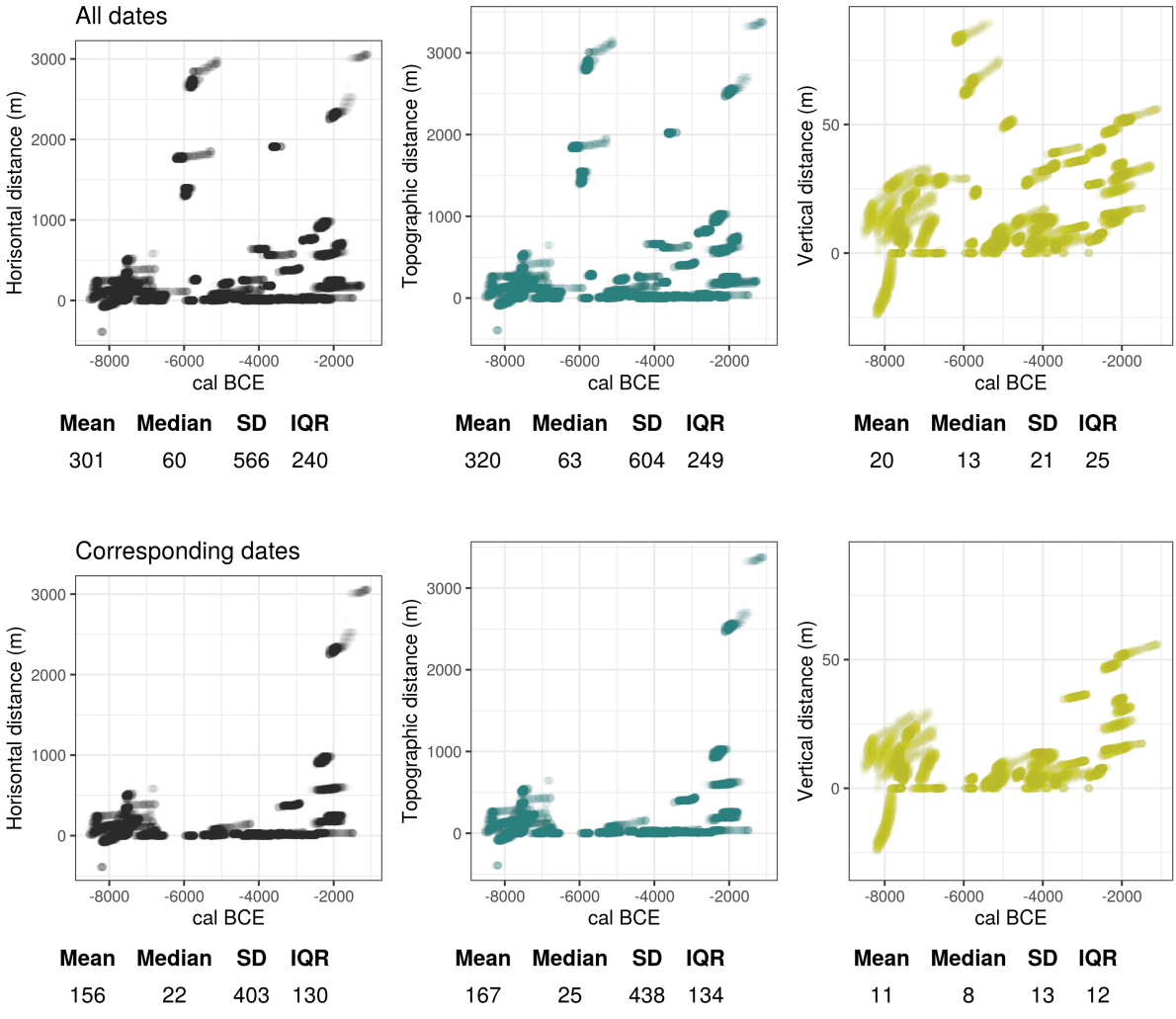

Figure 6: The result of running the analysis across all sites. Each data point is plotted with some transparency, meaning that the darker the colour, the more often those values occured. The first row shows the result of including all dates the Stone Age, including those seen as otherwise unrelated to the main occupation of the sites. The second row shows the result of excluding these. The table under each plot lists some corresponding statistics for central tendency and dispersion.

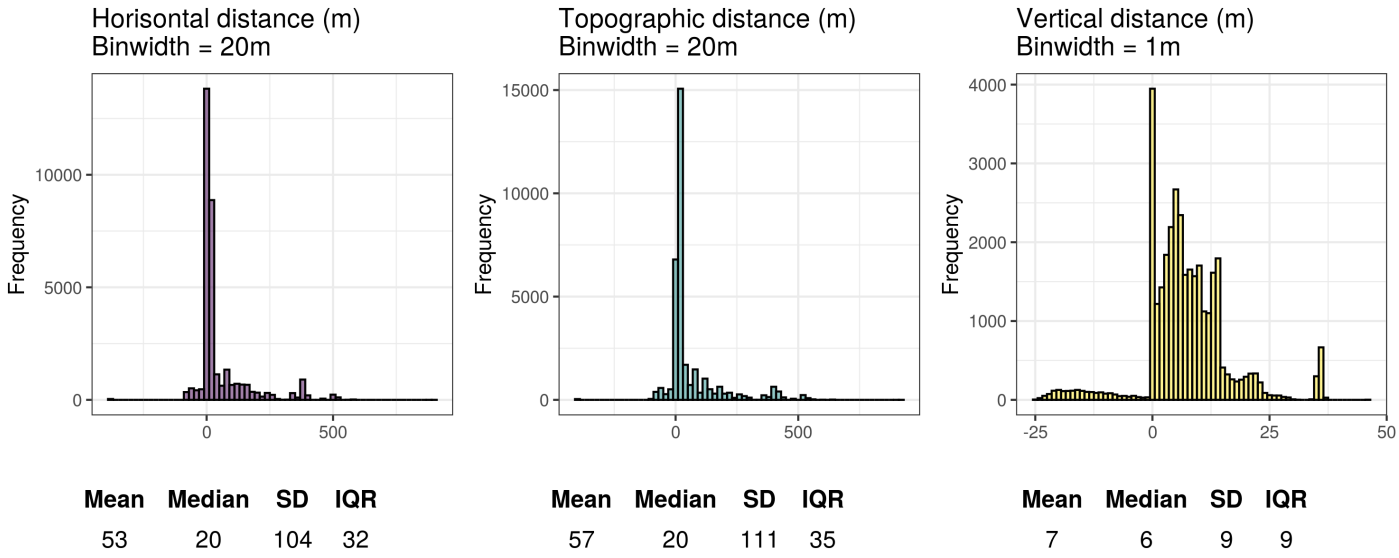

Figure 7: Histograms showing distance from shoreline using only dates older than 2500 BCE that correspond to the site inventory.

6 Discussion

Some sources of likely variation and uncertainty have not been considered here. First of all the DTM has only been corrected for major modern disturbances. This means that erosion, although likely not that prevalent, has not been taken into account. Secondly, the DTM has a vertical error... Thirdly, the tidal range has not been considered... Fourthly, the exposure of the sites to wave action is also likely to have been of concern, and will presumably have implications for how close to the shoreline people settled. And finally, the nature of the visits to the sites will presumably also have implications for how exposed a site

7 Conclusion

Here the approach was used to inform the question of the distance between sites and shorelines, but this method can be extended to a wide range of use-cases where one needs to visualise and quantitatively or qualitatively evaluate the relationship between archaeological phenomena, the prehistoric shore line, and the uncertainty inherent in this reconstruction.

8 References

Åstveit, L.I., 2018. The early mesolithic of western norway, in: Blankholm, H.P. (Ed.),. Equinox, Sheffield, pp. 231–274.

Berg-Hansen, I.M., 2009. Steinalderregistrering. Metodologi og forskningshistorie i norge 1900-2000 med en feltstudie fra lista i vest-agder. Museum of Cultural History, University of Oslo.

Bivand, R., 2021. rgrass7: Interface between GRASS 7 geographical information system and r. R package version 0.2-6.

Bjerck, H.B., 2008. Norwegian mesolithic trends: A review, in: Geoff, B., Spikins, P. (Eds.),. Cambridge University Press, Cambridge, pp. 60–106.

Bjerck, H.B., 2005. Strandlinjedatering. Pax, Oslo, pp. 363–364.

Bjerck, H.B., 1990. Mesolithic site types and settlement patterns at vega, northern norway. Acta Archaeologica 60, 1–32.

Breivik, H.M., Fossum, G., Solheim, S., 2018. Exploring human responses to climatic fluctuations and environmental diversity: Two stories from Mesolithic Norway. Quaternary International, Impacts of gradual and abrupt environmental changes on Late glacial to Middle Holocene cultural changes in Europe 465, 258–275. https://doi.org/10.1016/j.quaint.2016.12.019

Bronk Ramsey, C., 2009. Bayesian Analysis of Radiocarbon Dates. Radiocarbon 51, 337–360. https://doi.org/10.1017/S0033822200033865

Conolly, J., 2020. Spatial interpolation, in: Gillings, M., Hacıgüzeller, P., Lock, G. (Eds.),. Routledge, London & New York, pp. 118–134.

Conolly, J., Lake, M., 2006. Geographical information systems in archaeology. Cambridge University Press, Cambridge.

Crema, E.R., 2012. Modelling Temporal Uncertainty in Archaeological Analysis. Journal of Archaeological Method and Theory 19, 440–461. https://doi.org/10.1007/s10816-011-9122-3

Crema, E.R., Bevan, A., Lake, M.W., 2010. A probabilistic framework for assessing spatio-temporal point patterns in the archaeological record. Journal of Archaeological Science 37, 1118–1130. https://doi.org/10.1016/j.jas.2009.12.012

Fossum, G., 2020. Specialists facing climate change. The 8200 cal BP event and its impact on the coastal settlement in the inner oslo fjord, southeast norway, in: Schülke, A. (Ed.),. Routledge, London & New York, pp. 179–201.

Hafsten, U., 1983. Shore-level changes in South Norway during the last 13,000 years, traced by biostratigraphical methods and radiometric datings. Norsk Geografisk Tidsskrift - Norwegian Journal of Geography 37, 63–79. https://doi.org/10.1080/00291958308552089

Hafsten, U., 1957. De senkvartære strandlinje-forskyvningene i oslotrakten belyst ved pollenanalytiske undersøkelser. Norsk Geografisk Tidsskrift - Norwegian Journal of Geography 16, 74–99. https://doi.org/10.1080/00291955708622137

Hinz, M., Schmid, C., Knitter, D., Tietze, C., 2021. oxcAAR: Interface to 'OxCal' radiocarbon calibration. R package version 1.1.0.

Hughes, A.L.C., Gyllencreutz, R., Lohne, Ø.S., Mangerud, J., Svendsen, J.I., 2016. The last Eurasian ice sheets – a chronological database and time-slice reconstruction, DATED-1. Boreas 45, 1–45. https://doi.org/https://doi.org/10.1111/bor.12142

Jaksland, L., 2014. Kulturhistorisk sammenstilling, in: Jaksland, L., Persson, P. (Eds.),. University of Oslo, Museum of Cultural History, Oslo, pp. 11–46.

Lakens, D., Scheel, A.M., Isager, P.M., 2018. Equivalence Testing for Psychological Research: A Tutorial. Advances in Methods and Practices in Psychological Science 1, 259–269. https://doi.org/10.1177/2515245918770963

Lambeck, K., Smither, C., Ekman, M., 1998. Tests of Glacial Rebound Models for Fennoscandinavia Based on Instrumented Sea- and Lake-Level Records. Geophysical Journal International 135, 375–387. https://doi.org/10.1046/j.1365-246X.1998.00643.x.

Lewis, J., 2021. Probabilistic Modelling for Incorporating Uncertainty in Least Cost Path Results: a Postdictive Roman Road Case Study. Journal of Archaeological Method and Theory 28, 911–924. https://doi.org/10.1007/s10816-021-09522-w

MacCurdy, G.G., 1906. Review of strandliniens beliggenhed under stenalderen i det sydøstlige norge. Af w.

C. brøgger. Science 23, 778–780.
Marwick, B., Boettiger, C., Mullen, L., 2018. Packaging data analytical work reproducibly using r (and friends). The American Statistician 72, 80–88. https://doi.org/10.1080/00031305.2017.1375986
Milne, G.A., 2015. Glacial isostatic adjustment. Wiley, Chichester, pp. 421–437.
Milne, G.A., Gehrels, W.R., Hughes, C.W., Tamisiea, M.E., 2009. Identifying the causes of sea-level change. Nature Geoscience 2, 471–478. https://doi.org/10.1038/ngeo544
Mjærum, A., 2018. Hinterland discoveries: Middle Mesolithic woodland utilization and the case of the site Eidsberg, eastern Norway. Current Swedish Archaeology 26, 159–188. https://doi.org/10.37718/CSA.2018.11
Møller, J.J., 1987. Shoreline relation and prehistoric settlement in northern norway. Norwegian Journal of Geography 41, 45–60. https://doi.org/http://dx.doi.org/10.1080/00291958708552171
Mörner, N.-A., 1976. Eustasy and geoid changes. The Journal of Geology 84, 123–151. https://doi.org/10.1086/628184
Nummedal, A., 1923. Om flintpladsene. Norwegian Journal of Geography 7, 89–141.
Parnell, A.C., Haslett, J., Allen, J.R.M., Buck, C.E., Huntley, B., 2008. A flexible approach to assessing synchroneity of past events using Bayesian reconstructions of sedimentation history. Quaternary Science Reviews 27, 1872–1885. https://doi.org/10.1016/j.quascirev.2008.07.009
Prescott, C., 2020. Interpreting complex diachronic "neolithic" -period data in norway, in: Gron, K.J., Sørensen, L., Rowley-Conwy, P. (Eds.),. Oxbow Books, Oxford, pp. 381–400.
R Core Team, 2021. R: A language and environment for statistical computing. R Foundation for Statistical Computing, Vienna, Austria.
Reimer, P.J., Austin, W.E.N., Bard, E., Bayliss, A., Blackwell, P.G., Ramsey, C.B., Butzin, M., Cheng, H., Edwards, R.L., Friedrich, M., Grootes, P.M., Guilderson, T.P., Hajdas, I., Heaton, T.J., Hogg, A.G., Hughen, K.A., Kromer, B., Manning, S.W., Muscheler, R., Palmer, J.G., Pearson, C., Plicht, J. van der, Reimer, R.W., Richards, D.A., Scott, E.M., Southon, J.R., Turney, C.S.M., Wacker, L., Adolphi, F., Büntgen, U., Capano, M., Fahrni, S.M., Fogtmann-Schulz, A., Friedrich, R., Köhler, P., Kudsk, S., Miyake, F., Olsen, J., Reinig, F., Sakamoto, M., Sookdeo, A., Talamo, S., 2020. The IntCal20 Northern Hemisphere Radiocarbon Age Calibration Curve (0–55 cal kBP). Radiocarbon 62, 725–757. https://doi.org/10.1017/RDC.2020.41
Reitan, G., Berg-Hansen, I.M., 2009. Lundevågenprosjektet, delrapport 1. Sammenfattende rapport. Lunde, 6/1, 6/35 og skjolnes 7/23, 7/27, farsund kommune, vest-agder. Oslo.
Romundset, A., 2018. Postglacial shoreline displacement in the Tvedestrand-Arendal area, in: Reitan, G., Sundström, L. (Eds.), The Stone Age Coastal Settlement in Aust-Agder, Southeast Norway. Cappelen Damm Akademisk, Oslo, pp. 463–478.
Romundset, A., Bondevik, S., Bennike, O., 2011. Postglacial uplift and relative sea level changes in Finnmark, northern Norway. Quaternary Science Reviews 30, 2398–2421. https://doi.org/10.1016/j.quascirev.2011.06.007
Romundset, A., Fredin, O., Høgaas, F., 2015. A Holocene sea-level curve and revised isobase map based on isolation basins from near the southern tip of Norway 18.
Romundset, A., Lakeman, T.R., Høgaas, F., 2019. Coastal lake records add constraints to the age and magnitude of the Younger Dryas ice-front oscillation along the Skagerrak coastline in southern Norway. Journal of Quaternary Science 34, 112–124. https://doi.org/https://doi.org/10.1002/jqs.3085
Romundset, A., Lakeman, T.R., Høgaas, F., 2018. Quantifying variable rates of postglacial relative sea level fall from a cluster of 24 isolation basins in southern Norway. Quaternary Science Reviews 197, 175–192. https://doi.org/10.1016/j.quascirev.2018.07.041
Shennan, I., 2015. Handbook of sea-level research: Framing research questions. Wiley, Chichester, pp. 3–25.
Sognnes, K., 2003. On shoreline dating of rock art. Acta Archaeologica 74, 189–209.
Solheim, S., 2021. Timing the Emergence and Development of Arable Farming in Southeastern Norway by Using Summed Probability Distribution of Radiocarbon Dates and a Bayesian Age Model. Radiocarbon 1–22. https://doi.org/10.1017/RDC.2021.80
Solheim, S., 2020. Mesolithic coastal landscapes. Demography, settlement patterns and subsistence economy in southeastern norway, in: Schülke, A. (Ed.),. Routledge, London & New York.
Sørensen, R., 1999. En 14C datert og dendrokronologisk kalibrert strandforksyvningskurve for søndre østfold. Sørøst-norge, in: Selsing, L., Lillehammer, G. (Eds.), AmS-Rapport 12a. Museum of Archaeology,

Stavanger, pp. 227–242.
Sørensen, R., 1979. Late Weichselian deglaciation in the Oslofjord area, south Norway. Boreas 8, 241–246. https://doi.org/https://doi.org/10.1111/j.1502-3885.1979.tb00806.x
Sørensen, R., Henningsmoen, K.E., Høeg, H.I., Gälman, V., 2014a. Holocene landhevningsstudier i søndre vestfold og sørøstre telemark- revidert kurve, in: Melvold, S., Persson, P. (Eds.),. Portal, Kristiansand, pp. 36–47.
Sørensen, R., Høeg, H.I., Henningsmoen, K.E., Skog, G., Labowsky, S.F., Stabell, B., 2014b. Utviklingen av det senglasiale og tidlig preboreale landskapet og vegetasjonen omkring steinalderboplassene ved pauler, in: Jaksland, L., Persson, P. (Eds.), E18 Brunlanesprosjektet. Bind i. Forutsetninger Og Kulturhistorisk Sammenstilling. University of Oslo, Museum of Cultural History, Oslo, pp. 171–213.
Stroeven, A.P., Hättestrand, C., Kleman, J., Heyman, J., Fabel, D., Fredin, O., Goodfellow, B.W., Harbor, J.M., Jansen, J.D., Olsen, L., Caffee, M.W., Fink, D., Lundqvist, J., Rosqvist, G.C., Strömberg, B., Jansson, K.N., 2016. Deglaciation of Fennoscandia. Quaternary Science Reviews, Special Issue: PAST Gateways (Palaeo-Arctic Spatial and Temporal Gateways) 147, 91–121. https://doi.org/10.1016/j.quascirev.2015.09.016
Svendsen, J.I., Mangerud, J., 1987. Late Weichselian and holocene sea-level history for a cross-section of western Norway. Journal of Quaternary Science 2, 113–132. https://doi.org/10.1002/jqs.3390020205
Tallavaara, M., Pesonen, P., 2020. Human ecodynamics in the north-west coast of Finland 10,000–2000 years ago. Quaternary International 549, 26–35. https://doi.org/10.1016/j.quaint.2018.06.032
Wang, I., 2019. topoDistance: Calculating topographic paths and distances. R package version 1.0.1. Https://CRAN.r-project.org/package=topoDistance.

8.0.1 Colophon

This report was generated on 2021-12-07 20:07:48 using the following computational environment and dependencies:

```
#> - Session info  -------------------------------------------------------------
#>  hash: repeat button, woman health worker, prince: light skin tone
#>
#>  setting  value
#>  version  R version 4.1.2 (2021-11-01)
#>  os       Linux Mint 19.3
#>  system   x86_64, linux-gnu
#>  ui       X11
#>  language en_US
#>  collate  en_US.UTF-8
#>  ctype    en_US.UTF-8
#>  tz       Europe/Oslo
#>  date     2021-12-07
#>  pandoc   2.14.0.3 @ /usr/lib/rstudio/bin/pandoc/ (via rmarkdown)
#>
#> - Packages -----------------------------------------------------------------
#>  package      * version date (UTC) lib source
#>  assertthat     0.2.1   2019-03-21 [1] CRAN (R 4.1.0)
#>  backports      1.3.0   2021-10-27 [1] CRAN (R 4.1.2)
#>  BiocGenerics * 0.38.0  2021-05-19 [1] Bioconductor
#>  bitops         1.0-7   2021-04-24 [1] CRAN (R 4.1.0)
#>  bookdown       0.24    2021-09-02 [1] CRAN (R 4.1.1)
#>  broom          0.7.10  2021-10-31 [1] CRAN (R 4.1.2)
#>  cachem         1.0.6   2021-08-19 [1] CRAN (R 4.1.1)
#>  callr          3.7.0   2021-04-20 [1] CRAN (R 4.1.0)
#>  cellranger     1.1.0   2016-07-27 [1] CRAN (R 4.1.0)
#>  class          7.3-19  2021-05-03 [4] CRAN (R 4.0.5)
#>  classInt       0.4-3   2020-04-07 [1] CRAN (R 4.1.0)
#>  cli            3.1.0   2021-10-27 [1] CRAN (R 4.1.2)
#>  codetools      0.2-18  2020-11-04 [4] CRAN (R 4.0.3)
#>  colorspace     2.0-2   2021-06-24 [1] CRAN (R 4.1.0)
#>  crayon         1.4.2   2021-10-29 [1] CRAN (R 4.1.2)
#>  data.table     1.14.2  2021-09-27 [1] CRAN (R 4.1.2)
#>  DBI            1.1.1   2021-01-15 [1] CRAN (R 4.1.0)
#>  dbplyr         2.1.1   2021-04-06 [1] CRAN (R 4.1.0)
#>  desc           1.4.0   2021-09-28 [1] CRAN (R 4.1.2)
#>  devtools       2.4.2   2021-06-07 [1] CRAN (R 4.1.0)
#>  digest         0.6.28  2021-09-23 [1] CRAN (R 4.1.2)
#>  dplyr        * 1.0.7   2021-06-18 [1] CRAN (R 4.1.0)
#>  e1071          1.7-9   2021-09-16 [1] CRAN (R 4.1.2)
#>  ellipsis       0.3.2   2021-04-29 [1] CRAN (R 4.1.0)
#>  evaluate       0.14    2019-05-28 [1] CRAN (R 4.1.0)
#>  fansi          0.5.0   2021-05-25 [1] CRAN (R 4.1.0)
#>  farver         2.1.0   2021-02-28 [1] CRAN (R 4.1.0)
#>  fastmap        1.1.0   2021-01-25 [1] CRAN (R 4.1.0)
#>  forcats      * 0.5.1   2021-01-27 [1] CRAN (R 4.1.0)
#>  foreign        0.8-81  2020-12-22 [4] CRAN (R 4.0.3)
#>  fs             1.5.0   2020-07-31 [1] CRAN (R 4.1.0)
#>  gdistance      1.3-6   2020-06-29 [1] CRAN (R 4.1.1)
```

```
#>  generics       0.1.1   2021-10-25 [1] CRAN (R 4.1.2)
#>  ggmap          3.0.0   2019-02-05 [1] CRAN (R 4.1.1)
#>  ggnewscale   * 0.4.5   2021-01-11 [1] CRAN (R 4.1.1)
#>  ggplot2      * 3.3.5   2021-06-25 [1] CRAN (R 4.1.0)
#>  ggridges     * 0.5.3   2021-01-08 [1] CRAN (R 4.1.0)
#>  ggsn           0.5.0   2019-02-18 [1] CRAN (R 4.1.0)
#>  ggthemes     * 4.2.4   2021-01-20 [1] CRAN (R 4.1.1)
#>  glue           1.5.0   2021-11-07 [1] CRAN (R 4.1.2)
#>  gridExtra      2.3     2017-09-09 [1] CRAN (R 4.1.0)
#>  gtable         0.3.0   2019-03-25 [1] CRAN (R 4.1.0)
#>  haven          2.4.3   2021-08-04 [1] CRAN (R 4.1.1)
#>  here         * 1.0.1   2020-12-13 [1] CRAN (R 4.1.0)
#>  highr          0.9     2021-04-16 [1] CRAN (R 4.1.0)
#>  hms            1.1.1   2021-09-26 [1] CRAN (R 4.1.2)
#>  htmltools      0.5.2   2021-08-25 [1] CRAN (R 4.1.1)
#>  htmlwidgets    1.5.4   2021-09-08 [1] CRAN (R 4.1.1)
#>  httr           1.4.2   2020-07-20 [1] CRAN (R 4.1.0)
#>  igraph         1.2.8   2021-11-07 [1] CRAN (R 4.1.2)
#>  IRanges      * 2.26.0  2021-05-19 [1] Bioconductor
#>  jpeg           0.1-9   2021-07-24 [1] CRAN (R 4.1.0)
#>  jsonlite       1.7.2   2020-12-09 [1] CRAN (R 4.1.0)
#>  KernSmooth     2.23-20 2021-05-03 [4] CRAN (R 4.0.5)
#>  knitr          1.36    2021-09-29 [1] CRAN (R 4.1.2)
#>  labeling       0.4.2   2020-10-20 [1] CRAN (R 4.1.0)
#>  lattice        0.20-45 2021-09-22 [4] CRAN (R 4.1.1)
#>  lazyeval       0.2.2   2019-03-15 [1] CRAN (R 4.1.0)
#>  lifecycle      1.0.1   2021-09-24 [1] CRAN (R 4.1.1)
#>  lubridate      1.8.0   2021-10-07 [1] CRAN (R 4.1.2)
#>  magrittr       2.0.1   2020-11-17 [1] CRAN (R 4.1.0)
#>  maptools       1.1-2   2021-09-07 [1] CRAN (R 4.1.1)
#>  Matrix         1.3-4   2021-06-01 [4] CRAN (R 4.1.0)
#>  memoise        2.0.0   2021-01-26 [1] CRAN (R 4.1.0)
#>  modelr         0.1.8   2020-05-19 [1] CRAN (R 4.1.0)
#>  munsell        0.5.0   2018-06-12 [1] CRAN (R 4.1.0)
#>  oxcAAR       * 1.1.1   2021-07-05 [1] CRAN (R 4.1.0)
#>  patchwork    * 1.1.1   2020-12-17 [1] CRAN (R 4.1.0)
#>  pillar         1.6.4   2021-10-18 [1] CRAN (R 4.1.1)
#>  pkgbuild       1.2.0   2020-12-15 [1] CRAN (R 4.1.0)
#>  pkgconfig      2.0.3   2019-09-22 [1] CRAN (R 4.1.0)
#>  pkgload        1.2.3   2021-10-13 [1] CRAN (R 4.1.2)
#>  plotly         4.10.0  2021-10-09 [1] CRAN (R 4.1.2)
#>  plyr           1.8.6   2020-03-03 [1] CRAN (R 4.1.0)
#>  png            0.1-7   2013-12-03 [1] CRAN (R 4.1.0)
#>  prettyunits    1.1.1   2020-01-24 [1] CRAN (R 4.1.0)
#>  processx       3.5.2   2021-04-30 [1] CRAN (R 4.1.0)
#>  proxy          0.4-26  2021-06-07 [1] CRAN (R 4.1.0)
#>  ps             1.6.0   2021-02-28 [1] CRAN (R 4.1.0)
#>  purrr        * 0.3.4   2020-04-17 [1] CRAN (R 4.1.0)
#>  R6             2.5.1   2021-08-19 [1] CRAN (R 4.1.1)
#>  raster       * 3.5-2   2021-10-11 [1] CRAN (R 4.1.2)
#>  RColorBrewer   1.1-2   2014-12-07 [1] CRAN (R 4.1.0)
#>  Rcpp           1.0.7   2021-07-07 [1] CRAN (R 4.1.0)
#>  readr        * 2.1.0   2021-11-11 [1] CRAN (R 4.1.2)
#>  readxl         1.3.1   2019-03-13 [1] CRAN (R 4.1.0)
```

```
#>  remotes        2.4.1   2021-09-29 [1] CRAN (R 4.1.2)
#>  reprex         2.0.1   2021-08-05 [1] CRAN (R 4.1.1)
#>  rgdal          1.5-27  2021-09-16 [1] CRAN (R 4.1.2)
#>  RgoogleMaps    1.4.5.3 2020-02-12 [1] CRAN (R 4.1.0)
#>  rjson          0.2.20  2018-06-08 [1] CRAN (R 4.1.0)
#>  rlang          0.4.12  2021-10-18 [1] CRAN (R 4.1.1)
#>  rmarkdown      2.11    2021-09-14 [1] CRAN (R 4.1.2)
#>  rprojroot      2.0.2   2020-11-15 [1] CRAN (R 4.1.0)
#>  rstudioapi     0.13    2020-11-12 [1] CRAN (R 4.1.0)
#>  rvest          1.0.2   2021-10-16 [1] CRAN (R 4.1.2)
#>  s2             1.0.7   2021-09-28 [1] CRAN (R 4.1.2)
#>  S4Vectors    * 0.30.0  2021-05-19 [1] Bioconductor
#>  scales         1.1.1   2020-05-11 [1] CRAN (R 4.1.0)
#>  sessioninfo    1.2.1   2021-11-02 [1] CRAN (R 4.1.2)
#>  sf           * 1.0-4   2021-11-14 [1] CRAN (R 4.1.2)
#>  sp           * 1.4-6   2021-11-14 [1] CRAN (R 4.1.2)
#>  stringi        1.7.5   2021-10-04 [1] CRAN (R 4.1.1)
#>  stringr      * 1.4.0   2019-02-10 [1] CRAN (R 4.1.0)
#>  terra        * 1.4-19  2021-11-15 [1] CRAN (R 4.1.2)
#>  testthat       3.1.0   2021-10-04 [1] CRAN (R 4.1.2)
#>  tibble       * 3.1.6   2021-11-07 [1] CRAN (R 4.1.2)
#>  tidyr        * 1.1.4   2021-09-27 [1] CRAN (R 4.1.2)
#>  tidyselect     1.1.1   2021-04-30 [1] CRAN (R 4.1.0)
#>  tidyverse    * 1.3.1   2021-04-15 [1] CRAN (R 4.1.0)
#>  topoDistance * 1.0.1   2019-08-02 [1] CRAN (R 4.1.1)
#>  tzdb           0.2.0   2021-10-27 [1] CRAN (R 4.1.2)
#>  units          0.7-2   2021-06-08 [1] CRAN (R 4.1.0)
#>  usethis        2.1.3   2021-10-27 [1] CRAN (R 4.1.2)
#>  utf8           1.2.2   2021-07-24 [1] CRAN (R 4.1.0)
#>  vapour       * 0.8.5   2021-10-07 [1] CRAN (R 4.1.2)
#>  vctrs          0.3.8   2021-04-29 [1] CRAN (R 4.1.0)
#>  viridis        0.6.2   2021-10-13 [1] CRAN (R 4.1.2)
#>  viridisLite    0.4.0   2021-04-13 [1] CRAN (R 4.1.0)
#>  withr          2.4.2   2021-04-18 [1] CRAN (R 4.1.0)
#>  wk             0.5.0   2021-07-13 [1] CRAN (R 4.1.0)
#>  xfun           0.28    2021-11-04 [1] CRAN (R 4.1.2)
#>  xml2           1.3.2   2020-04-23 [1] CRAN (R 4.1.0)
#>  yaml           2.2.1   2020-02-01 [1] CRAN (R 4.1.0)
#>
#>  [1] /home/isak/R/x86_64-pc-linux-gnu-library/4.1
#>  [2] /usr/local/lib/R/site-library
#>  [3] /usr/lib/R/site-library
#>  [4] /usr/lib/R/library
#>
#> ------------------------------------------------------------------------------
```

The current Git commit details are:

```
#> Local:    master /home/isak/phd/assessing.sealevel.dating
#> Remote:   master @ origin (https://github.com/isakro/assessing.sealevel.dating.git)
#> Head:     [e377448] 2021-12-04: Writing through supplementary
```